Sensors & Transducers, Vol. 185, Issue 2, February 2015, pp. 156-161

www.sensorsportal.com

Sensors & Transducers

http://www.sensorsportal.com

On the Usage of Cyclic Voltammetry and Impedance Spectroscopy for Measuring the Concentration of Aqueous Solutions

Manuel Fiedler, Ingo Tobehn, Andrea Cyriax, Heike Wünscher, Arndt Steinke, Thomas Frank

Mikrosensorik und Photovoltaik GmbH, Konrad-Zuse-Straße 14, 99099 Erfurt, Germany
Tel.: +49 361 663 1410, fax: +49 361 663 1413
E-mail: cis-mems@cismst.de

Received: 14 November 2014 /Accepted: 15 January 2015 /Published: 28 February 2015

Abstract: This article describes sensors for concentration measurement based on the electro-chemical properties of the liquid being measured. Herein two electrical methods, namely cyclic voltammetry and impedance spectroscopy, are being presented. The measurement can be performed quasi simultaneously using the same measurement medium. Further optimization of the combined methods is possible by adapting the geometric design of the electrode structure, the electrode material, the optional passivation and the electric coupling (galvanically or capacitively). In summary, by combining multiple sensory principles on a device it becomes possible to analyze mixtures of substances contained in a solution with respect to their composition. *Copyright © 2015 IFSA Publishing, S. L.*

Keywords: Interdigital structure, Impedance spectroscopy, Cyclic voltammetry, Silicon.

1. Introduction

Sensors for concentration measurements are a very vast area of research. A concentration measurement is used when the components are known, but not their content. For their determination several substance-specific sensor principles are known. In this article, two electrical methods are presented using the implementation as the sensing element is reported [1].

These methods are based on cyclic voltammetry and impedance spectroscopy. In cyclic voltammetry a rising and then sloping current is applied between the working electrode and the counter electrode in a solution. The potential is determined by a reference electrode. If there is a redox-active substance in the solution, it will be oxidized or reduced at a characteristic potential. The current is recorded as a function of voltage. The voltage in the oxidation and reduction and the corresponding maximum current are of interest. Impedance spectroscopy detects both the dielectric properties of a medium and its conductivity as a function of frequency. In aqueous solution, these properties are dependent on the concentration.

The base of the sensors is an interdigital structure. Fig. 1 shows different variations of designs. The main features can be combined freely. A galvanic or capacitive coupling is possible. The DUT (device under test) can be a liquid or a solid. The organic or inorganic sensitive solid is applied directly to the sensor surface. The thickness is only a few 100 nm and is micro- or nano-porous. This binds substances (DUT) by absorption from the surrounding

atmosphere, such as water or carbon dioxide. The electrical properties change due to this and are determined by the spectroscopy. Table 1 shows the different materials for the sensor.

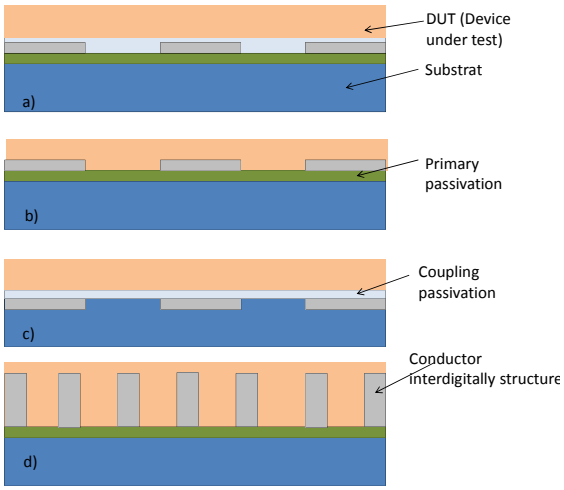

Fig. 1. Various design options a) interdigital structure, passivated for a capacitive coupling; b) interdigitated structure without passivation, galvanic coupling, c) implanted in silicon interdigital structure, d) 3D interdigital structure.

Table 1. Optional Materials for the Sensor.

Base material	**Silicon, (optional) Borosilica**
Passivation Base material	SiO_2
Conductor	Doped Silicon, MoSi, Gold Platinum
Passivation Conductor (optional)	Si_3N_4, ZrO_2, Al_2O_3 (20 nm to 500 nm)

A more detailed view of the construction can be seen in Fig. 2, a cut-through of an interdigital structure without passivation. The most important geometrical parameters for the sensor are the channel height (H1), the channel width (V3) and the size of the gap (V2). In case of an interdigital structure with passivation, an additional parameter is the thickness of passivation. The structure was etched by ICP (Inductively coupled plasma).

When choosing these parameters, several influences have to be taken into consideration. A higher channel width decreases the resistance of the channel as well as the overall capacitance by decreasing the number of channels per square millimeter. A wider gap reduces the capacitance between the channels and makes it easier for liquids to flow into the channel.

In addition to the measurement of purely chemical parameters, such as concentration, measurement of biological media is possible. The evaluation of the measurement results, however, requires great experience. In [2] and [3], the dielectric measurement of a biological medium is described by some examples.

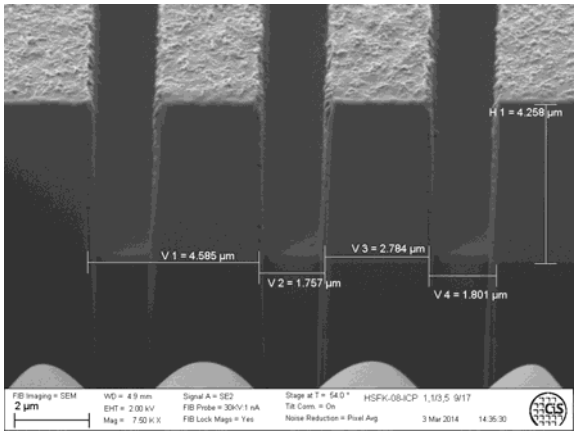

Fig. 2. FIB cross-sections and SEM image of a 3D interdigital structure. Doped polysilicon to 2 microns silicon dioxide layer.

Often the signal is not very selective on the type of material. In the DUT the selectivity of the sensor can be increased adding an indicator; using the mixing ratio and the associated change in impedance even a multi-component system can be analyzed. Further optimization of the combined methods is possible by the geometric design of the electrode structure, the electrode material, the optional passivation and the electric coupling.

The combination of multiple sensory principles on a device can be used to analyze a multicomponent system with a simple sensor.

2. Experimental Setup

For the evaluation and adaptation of the sensor's design, a test setup was constructed. The design is configured such that the distances can be selected in a range of 200 microns with free a resolution of 5 microns. In Fig. 3, the measuring principle is shown. By choosing the connections of the electrode gap can be selected. In [2] and [3], this method is described in detail.

The measurement setup for impedance spectroscopy can be seen in Fig. 4. Here, the analysis-chip with the interdigital structure on it is seen in the middle. It is surrounded by 12 dual multiplexer, which can be used to select the 24 measurement channels (12 per page). On the left side of the figure there are SMA connectors for connecting an external LCR meter to chip, with which the impedance of the device can be measured.

Fig. 5 shows the sensor for the combined impedance spectroscopy and cyclic voltammetry. With the aid of a multiplexer array, a line-bound connection between the measuring object and the impedance spectrometer is established. Subsequently,

the impedance spectroscopy is performed for the selected channel.

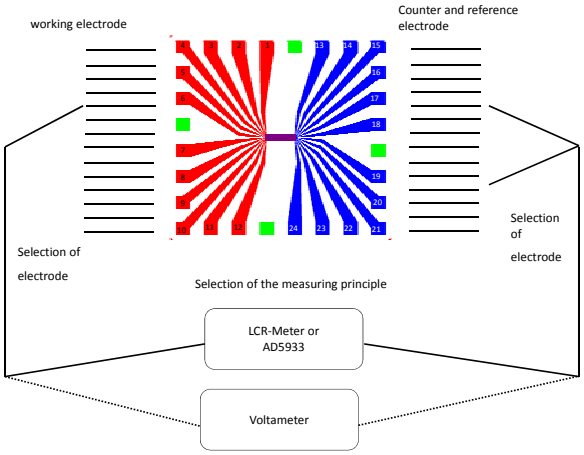

Fig. 3. The principle for the combined impedance spectroscopy and cyclic voltammetry.

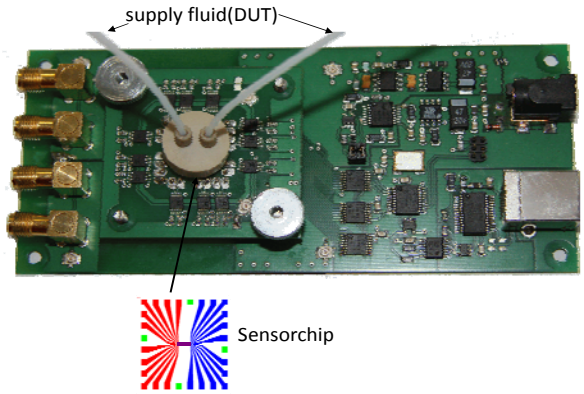

Fig. 4. The electronic circuit for the combined impedance spectroscopy and cyclic voltammetry with die connector for the fluid.

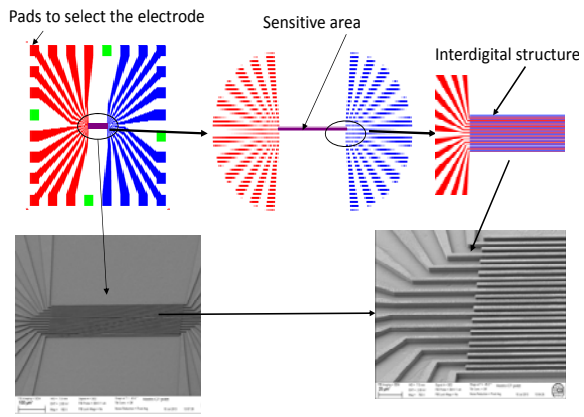

Fig. 5. The sensor for the combined impedance spectroscopy and cyclic voltammetry.

Through the recess in the middle, the liquid which is to be investigated can be applied to the interdigital structure either directly, or a flow chamber can be installed to then perform the impedance spectroscopy using the desired channels.

3. Measurements for Evaluation

For the evaluation and calibration of the sensor measurements are performed on an aqueous solution of KCl, ranging from 0.00002 mol/l to 1 mol/l. Fig. 6 shows the frequency dependent measurement of the impedance |Z| of the aqueous KCl solution, the distance between the electrodes is constant. In Fig. 7 the result when measurement is being performed at different distances of the electrodes is shown. In this way, the appropriate geometric structure is found for the measuring task.

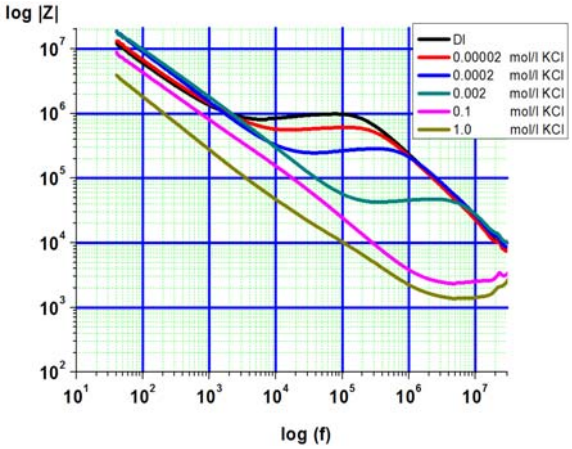

Fig. 6. Concentration measurement, variation in the concentration.

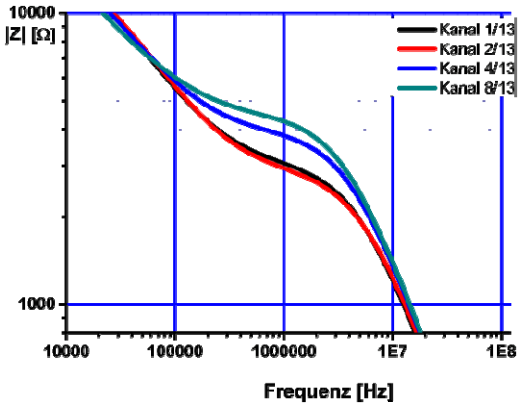

Fig. 7. Concentration measurement, variation of the electrode distance.

With the aid of the measured values, the amount and phase |Z|, an equivalent circuit diagram is developed. The values for the components are determined by a curve fitting. The results are shown in the Fig. 8. The equivalent circuit is now allows for the calculation of the resistor R1 from the measured values and the calibration of the sensor to the

conductance. Fig. 9 shows the graph of the curve fitting. In Fig. 10 the resistances as a function of concentration from the curve fitting are plotted.

Parameters	Upper Limit	Lower Limit	Result/In.Val.	Error %	Fix
C1	6.7785e-13	6.7785e-13	6.7785E-13	1.016	☑
R1	1000000	0	2.4802E05	3.7676	☐
P1	0.0005	0	5.2288E-10	3.7702	☐
n1	1	0	0.83005	0.51933	☐

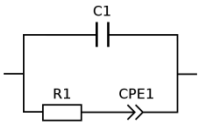

Fig. 8. Equivalent circuit diagram and the curve fitting.

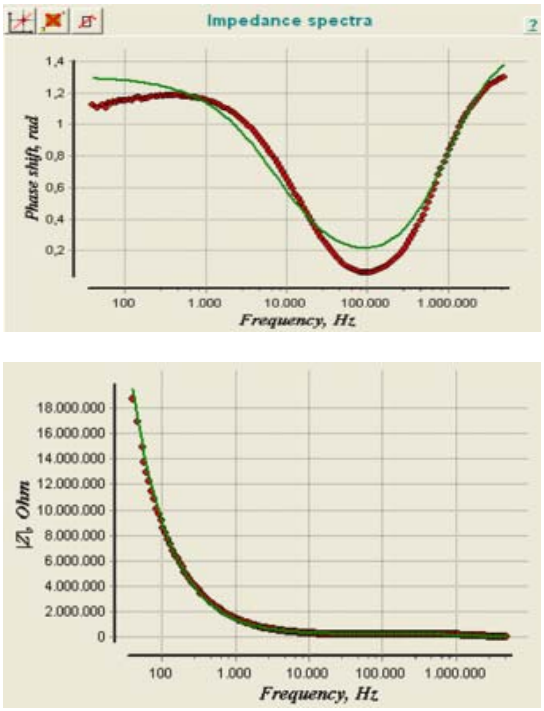

Fig. 9. Graph of the curve fitting.

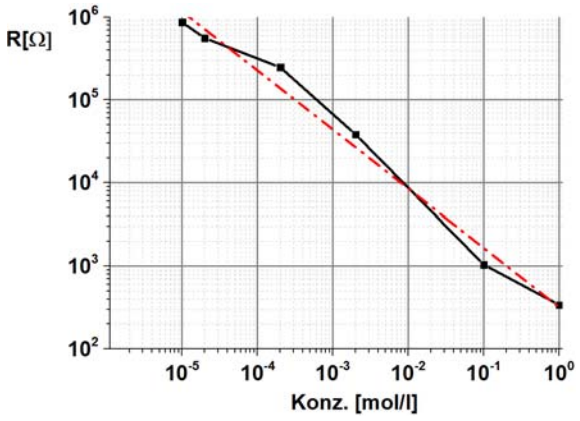

Fig. 10. Concentration measurement, variation of the electrode distance.

Various layer structures, geometries and measurement strategies are explored. The aim is to explore a multi-component system with various sensors at the same location. The concentration of the components is derived from the signal pattern. If the sensor is calibrated, the concentration of the ingredients can be determined from the signal pattern. One application is the in-line measurement in biogas plants to optimize the output.

[4-6] give an overview of the previous work done. The cyclic voltammetry is partially used in micro-sensors, but not in combination with the impedance spectroscopy. The essential idea and novelty are related to the connection of several measurement principles and sensitivities to determine the concentration at the same location. In summary, by combining multiple sensory principles on a device it becomes possible to determine the composition of substances contained in solution.

4. Sensor Arrangement for Measuring the Permittivity

For the measurement task, the determination of the Permittivity of different liquids, the design shown in Fig. 1 was evaluated.

If the sensor is to be used in order to determine the permittivity of a liquid, an application has to be found which separates the influence of the permittivity from the influence of other parameters. The permittivity mostly influences the direct capacity (C1 in Fig. 8). Therefore the sensor has to be operated within a frequency-range where C1 dominates. One example of this can be seen in Fig. 11, showing a 3D interdigital structure etched by etched by ICP.

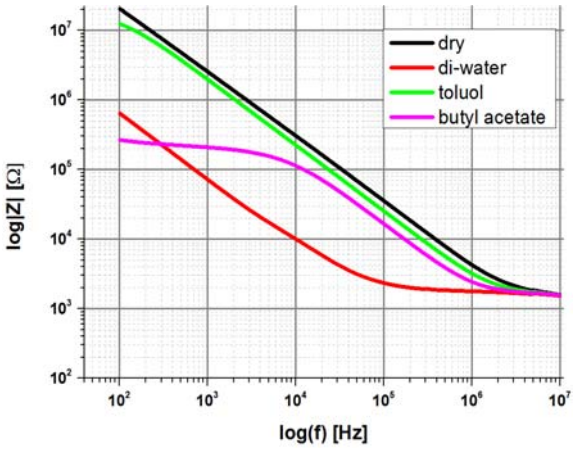

Fig. 11. Frequency-dependencies of a Fig. 1d sensor for different fluids.

As can be seen, the sensor has a region starting roughly around 10 kHz and ending around 100 kHz wherein the sensor shows solely the influence of C1.

Using this, the value of C1 can be estimated. The dependency of the capacitance from the permittivity is displayed in Fig. 12.

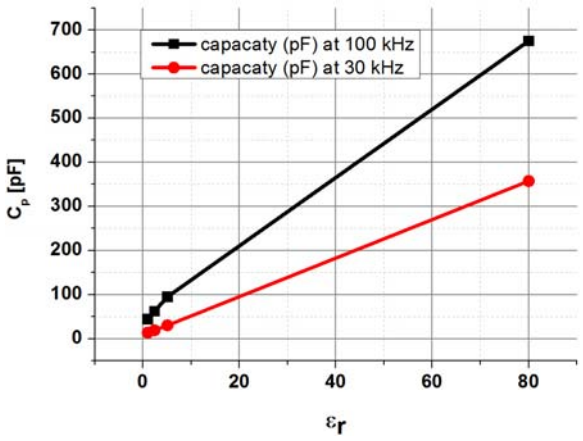

Fig. 12. Permittivity vs. capacitance at 100 kHz.

In order for a Sensor to be usable for this type of Measurement, the region in which C1 dominates has to be clearly distinguishable from the other regions and within a range of measurable parameters. This is clearly not always the case. Some sensors, like those with Ti02 passivization, show no real ability do tell the different regions apart. As seen in Fig. 13, the C1 dominated region for toluol starts at approximately 30 kHz, while the region for deionized water ends at approximately 20 kHz, giving no overlap for the whole range.

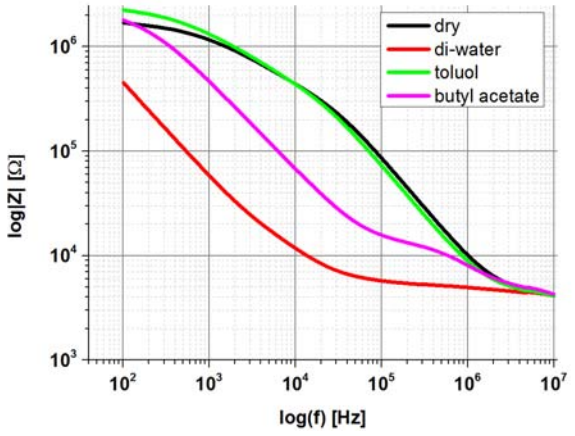

Fig. 13. Frequency-dependencies of a sensor with 20 nm TiO2 passivization for different fluids.

Other chips, such as an interdigital structure, passivated for a capacitive coupling (Fig. 1a), with an electrical resistivity of > 300 Ωcm show little differences between the varying fluids at all. This becomes evident when the graph in Fig. 14 is analyzed. Hereby the change in signal from ε=1 to ε=80 is less than 2 %. Therefore, the sensor is not feasible for this kind of measurement application.

When deciding the applicability of a sensor for measuring the permittivity, there are mainly three important aspects to consider (Fig. 8):

1. C1 should be relatively big
2. The quotient CPE1/C1 should be as big as possible
3. The resistance R1 should be as small as possible

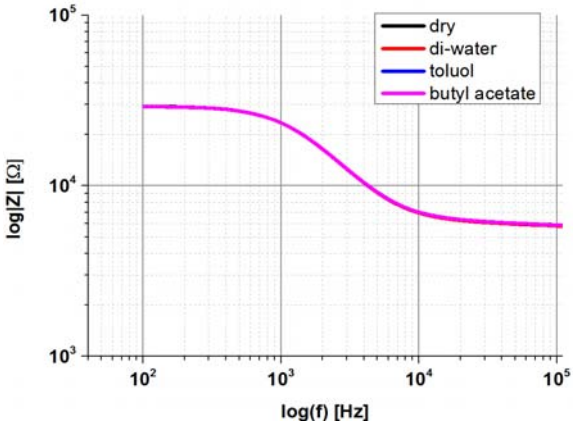

Fig. 14. Frequency-dependencies of sensor like a Fig. 1a (interdigital structure, passivated for a capacitive coupling) for different fluids.

The results of these changes can be seen in Fig. 15. Since the sensor with a 1.1 µm raster has a higher capacitance than the one with a 1.3 µm raster, a steeper gradient is observed. On the other hand, a higher overall capacitance lovers the coefficient of determination, since it less strongly separates the different influences.

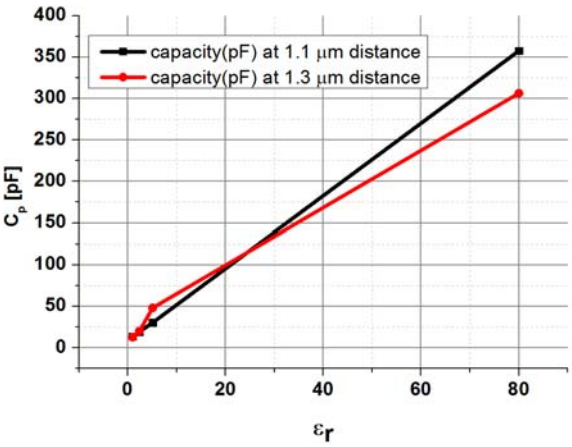

Fig. 15. Permittivity vs. capacitance at 30 kHz.

5. Experiments on the Ternary System Water-acetic Acid-propionic Acid

The ratio of acetic acid-propionic acid is a control parameter for the operation of biogas plants [7]. The sequence of processes in biogas plants is not

explained here, an intrigued reader might take a look at [8]. The concentration measurement in this mixture is very challenging because acetic acid and propionic acid share similar chemical properties. The separate determination of the concentration of acetic acid and propionic acid in the mixture of the two materials is difficult because both materials differ structurally only by an additional-CH2-group, which is insignificant in terms of responsiveness and many physical properties.

Cyclic voltammetry is preferably used to investigate redox processes in terms of their mechanism. It turns the electrode material used as a limit to the administrable voltage. Since acetic and propionic acid can be reduced only under very drastic conditions to the aldehyde, it can be expected that the cyclic voltammetry for the quantitative determination of these two components provides no useful results.

For the same reason, actually, no significant differences in the dielectric properties of both substances in the impedance spectroscopy arise. A variety of electrochemical processes are modeled in the equivalent circuit with a CPE (constant phase element). This reflects the ion mobility in the solution, which also depends on the mass of the moving particle. Thus the different molar masses of acetic and propionic-acid could be used for the analysis in this way. In Table 2, the two substances are shown.

R1 and C3 in this case represent the influence of the used multiplexer on the recorded spectra, while the remaining elements result from the properties of the comb structure used and of the measured liquid. First results show the practicability of this method. In addition, by varying the electrode spacing, all the other parameters which are characteristic of the liquid can be varied in order to eliminate them by a subsequent subtraction.

Table 2. Comparison of acetic acid and propionic acid.

	Acetic acid	**Propionic acid**
	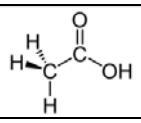	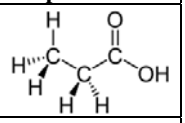
Molmass (g mol^{-1})	60.05	74.08
pK$_s$	4.76	4.87
Refractive index	1.371	1.386

Acknowledgment

We thank the Bundesministerium für Bildung und Forschung (BMBF) and the Projektträger Jülich (PtJ), the support for this project, Modellbasierte Prozess-steuerung von Biogasanlage (Förderkennzeichen 035F0456C) financially.

References

[1]. Th. Frank, I. Tobehn, A. Cyriax, M. Fiedler, A. Steinke, Sensor platform for measuring the concentration in aqueous solutions by cyclic voltammetry and impedance spectroscopy, in *Proceedings of the 5th International Conference on Sensor Device Technologies and Applications (SENSORDEVICES'14),* Lissabon, Portugal, 16-20 November 2014, pp.123-126.

[2]. M. Westenthanner, A. Barthel, P. He, D. Beckmann, A. Steinke, I. Tobehn, U. Pliquett, Assessment of suspension medium conductivity by means of micro electrodes, *Journal of Physics: Conference Series*, Vol. 434, No. 1, April 2013, pp. 012025-012093.

[3]. U. Pliquett, E. Gersing, F. Pliquett, Evaluation of Fast Time-domain Based Impedance Measurements on Biological Tissue, *Biomed Technik*, Vol. 45, No. 1, 2000, pp. 6-13.

[4]. L. Wahn, H. K. Trieu, L. Behrendt, S. Hemanth, Kohlenstoffdotierter Fotolack als Elektrodenmaterial für die in-situ Messung von Nitrit, in *Proceedings of the Conference on Mikrosystemtechnik Kongress*, Germany, 2013.

[5]. A. Rösner, Th. Frank, I. Tobehn, Bio instrument for determining the viability of cells on the basis of the impedance measurement, in *Proceedings of the Conference on Micromechanics and Microsystems Europe (MME'12)*, Ilmenau, Germany, 09-12 September 2012.

[6]. H. E. Ayliffe, A. Bruno Frazier, R. D. Rabbitt, Electric impedance spectroscopy using microchannels with integrated metal electrodes, *Journal of Microelectromechanical Systems,* Vol. 8, No. 1, March 1999, pp. 50-57.

[7]. College Leipzig Web Portal (https://fbme.htwk-leipzig.de/fileadmin/fbme/professoren/jung/propionsaeure_uwe_jung.pdf).

[8]. PFI Biotechnology Web Portal (http://pfi-biotechnology.de/fileadmin/templates/PFI_Biotechnology/Abschlussbericht_FNR_Propionsaeure2011-06-30.pdf).

[9]. Th. Frank, I. Tobehn, A. Steinke, S. Päßler, W. Fichtner, Electric impedance spectroscopy using microchannels with integrated metal electrodes, in *Proceedings of the 14th International Meeting on Chemical Sensors (IMCS'12)*, Nürnberg, Germany, 20-23 May 2012.